Sensitivity of Constrained Linear Inversions to the Selection of the Lagrange Multiplier

MICHAEL D. KING

Laboratory for Atmospheric Sciences, Goddard Space Flight Center, NASA, Greenbelt, MD 20771

(Manuscript received 10 June 1981, in final form 28 January 1982)

ABSTRACT

The sensitivity of constrained linear inversions to the selection of the Lagrange multiplier is demonstrated for the case of inferring columnar aerosol size distributions from spectral aerosol optical depth measurements. Since negative values of the aerosol size distribution constitute an unphysical solution, the Lagrange multiplier is varied within a restricted range until a range of values is reached for which all elements of the solution vector are positive. In addition to the constraint that the solution vector be positive, it is necessary for the final solution to be a smooth function and to satisfy the original integral equation to within the noise level of the measurements. An iterative method is presented whereby an initial estimate of the size distribution is modified until the final solution satisfies both the positivity constraint and the requirement that the regression fit to the data using the inverted size distribution be consistent with the measurement errors. A formula for calculating the variances and covariances in the inversion solution is derived and applied to optical depth measurements obtained at the University of Arizona and at Goddard Space Flight Center. In the former case an estimate of the measurement errors is available and thus the inversion formula and error analysis explicitly includes the magnitudes of the measurement variances. In the latter case the measurement errors are not known and the analysis assumes the errors in the measurements are equal and uncorrelated. Results of the error analysis show that the variances in the solution vector are large for radii where the information content of the measurements is small.

1. Introduction

Inversion methods for solving Fredholm integral equations of the first kind have existed for some 20 years. The earliest method for solving these indirect sensing problems in which due consideration was given to the estimation problem was the linear inversion technique developed by Phillips (1962) and Twomey (1963). This inversion method, which was arrived at independently by Tikhonov (1963), is commonly referred to as constrained linear inversion because it relies on the introduction of an additional condition or constraint, not deriving from the measurements, which enables one of the set of possible solution vectors to be selected. Many applications of constrained linear inversion can be found in the literature. These include the inference of atmospheric temperature profiles from satellite-borne radiometers (Wark and Fleming, 1966; Glasko and Timofeyev, 1968a,b), inference of the vertical distribution of ozone from scattered sunlight (Yarger, 1970), and the inference of aerosol size distributions from spectral attenuation (Yamamoto and Tanaka, 1969; King *et al.*, 1978; Walters, 1980) or angular light scattering (Dave, 1971; Byrne, 1978; Reagan *et al.*, 1980) measurements.

In each of these problems, as in any physics or engineering problem involving Fredholm integral equations of the first kind, the measurements and frequently the kernel functions are known with only finite accuracy. In addition, there is often a high degree of interdependence among some of the kernel functions which leads to highly oscillatory and unsatisfactory solutions in the absence of a suitable constraint. In a Bayesian sense this arises from a vague prior knowledge of the solution vector $f(x)$ in that least-squares assumes only that $-\infty < f(x) < \infty$ for all values of x. For most problems likely to be encountered in the atmospheric sciences, such as those outlined above, this range for $f(x)$ is unnecessarily broad since physical necessity dictates that the solution vector must at the very least be positive.

In addition to the constraint that the solution vector be positive, it is normal to seek the solution among the set of possible solutions which is the smoothest in some sense. Phillips (1962) introduced a smoothing constraint such that the sum of the squares of the second derivatives of the solution points is minimized. Twomey (1977) discusses many possible constraints that can be applied in constrained linear inversion problems, but Phillips' second derivative smoothing constraint remains one of the most popular in the atmospheric sciences. Among mathematicians the most popular constraint is that the sum of the squares of the solution points is minimized. This leads to the constraint matrix being the identity matrix and is referred to by Hoerl and Kennard (1970a,b) as ridge regression, rather than con-

strained linear inversion. The formulation of the problem as one in which a non-negative Lagrange multiplier is introduced as a means of varying the relative contribution of the kernel matrix and the constraint matrix remains the same.

The intent of this paper is to demonstrate the sensitivity of constrained linear inversions to the selection of the Lagrange multiplier and to demonstrate how one can obtain useful solutions in inversion problems by appropriately selecting the proper value (or values) of the Lagrange multiplier. The problem of inferring columnar aerosol size distributions from spectral optical depth measurements has been chosen as an example, though the methods to be presented are applicable to a much larger class of problems. A formula for calculating variances and covariances in the inversion solution is derived and applied to optical depth measurements obtained at the University of Arizona and at Goddard Space Flight Center.

2. Constrained linear inversion

Many remote sensing problems can be expressed in the form

$$g(y) = \int_a^b K(x, y)f(x)dx, \tag{1}$$

where the function $g(y)$ is measured and the indicial function $f(x)$ is to be inferred. In very few inversion problems can an expression for $f(x)$ be written analytically as a function of $g(y)$, and thus a numerical approach must be followed. Phillips (1962) argued that in any practical problem the Fredholm integral equation of the first kind should be rewritten as

$$g(y) = \int_a^b K(x, y)f(x)dx + \epsilon(y), \tag{2}$$

where the function $\epsilon(y)$ arises from measurement errors as well as any uncertainties as to the exact form of the kernel function $K(x, y)$. If we measure $g(y)$ at p discrete values of y, and wish to infer $f(x)$ at q discrete values of x, a system of linear equations results which may be written as

$$\mathbf{g} = \mathbf{A}\mathbf{f} + \boldsymbol{\epsilon}. \tag{3}$$

In this expression $\mathbf{A}$ is a $p \times q$ matrix representation of the kernel function which contains weighting factors whose values depend on the quadrature formula used. Although quadrature errors can contribute to the magnitude of the unknown error vector $\boldsymbol{\epsilon}$, the difficulties encountered in inversion problems are seldom caused by a loss of accuracy in going from an integral to a finite sum (Twomey, 1977).

It is well known that the inverse problem in which the Fredholm integral equation expressing radiation $g(y)$ as a function of the atmospheric state $f(x)$ is inverted to express the atmospheric state in terms of radiation is ill-posed, i.e., there is no mathematically unique solution. This led Phillips (1962) to the estimation problem in which a set of appropriate criteria are introduced in order to determine the best and most physical solution among the family of solutions which satisfy (3). Twomey (1977) showed that Phillips' constraint in which the sum of the squares of the second derivatives of the solution points is minimized is only one of many measures of smoothness which can be selected, and that the measure of smoothness can in general be written as $\mathbf{f}^T\mathbf{H}\mathbf{f}$, where $\mathbf{H}$ is usually a simple near-diagonal matrix and where superscript T denotes matrix transposition. The solution vector $\mathbf{f}$ is then obtained by minimizing a performance function Q, defined as

$$Q = Q_1 + \gamma Q_2, \tag{4}$$

where

$$Q_1 = \boldsymbol{\epsilon}^T\mathbf{S}_\epsilon^{-1}\boldsymbol{\epsilon} = \sum_{i=1}^{p}\sum_{j=1}^{p} \epsilon_i S_{\epsilon ij}^{-1}\epsilon_j, \tag{5}$$

$$Q_2 = \mathbf{f}^T\mathbf{H}\mathbf{f} = \sum_{i=1}^{q}\sum_{j=1}^{q} f_i H_{ij} f_j. \tag{6}$$

In these expressions γ is a non-negative Lagrange multiplier and $\mathbf{S}_\epsilon$ the measurement covariance matrix. This follows from the Gauss-Markov theorem (see, e.g., Liebelt, 1967) and thus the minimum value of Q represents the statistically optimum estimate of $\mathbf{f}$.

The solution vector $\mathbf{f}$ for which (4) is a minimum is readily shown to be

$$\mathbf{f} = (\mathbf{A}^T\mathbf{S}_\epsilon^{-1}\mathbf{A} + \gamma\mathbf{H})^{-1}\mathbf{A}^T\mathbf{S}_\epsilon^{-1}\mathbf{g}. \tag{7}$$

For the case in which the statistical errors in the measurements are assumed equal and uncorrelated, $\mathbf{S}_\epsilon$ reduces to $s^2\mathbf{I}$, where s^2 represents the sample variance for the regression fit and $\mathbf{I}$ is the identity matrix. With this assumption, Eq. (7) reduces to the familiar form derived by Twomey (1963), given by

$$\mathbf{f} = (\mathbf{A}^T\mathbf{A} + \gamma\mathbf{H})^{-1}\mathbf{A}^T\mathbf{g}, \tag{8}$$

where s^2 has been incorporated into the magnitude of γ.

Equations equivalent to (7) have been derived or applied by Liebelt (1967), Strand and Westwater (1968), Westwater and Strand (1968), Rodgers (1970, 1971) and DeLuisi and Mateer (1971) in the context of statistical estimation theory, and King *et al.* (1978) and Twomey (1977) in the context of constrained linear inversion. In the former case $\gamma\mathbf{H}$ is replaced by the inverse of an *a priori* estimate of the solution covariance matrix, and in this sense serves the same purpose as the constraint matrix and the undetermined Lagrange multiplier (Rodgers, 1976).

In applying either (7) or (8) to the solution of the inverse problem it is necessary to select a value for γ. Many different methods have been used for determining the Lagrange multiplier. Yarger (1970)

and Dave (1971) based their selection of γ on the magnitude of the maximum eigenvalue of $\mathbf{A}^T\mathbf{A}$ since, for the special case where $\mathbf{H}$ equals the identity matrix $\mathbf{I}$, the eigenvalues of $\mathbf{A}^T\mathbf{A} + \gamma\mathbf{I}$ are simply the eigenvalues of $\mathbf{A}^T\mathbf{A}$ incremented by γ. This is a useful method for understanding the nature of the constraint but it does not guarantee either positive solutions or permit easy extension to other forms of the $\mathbf{H}$ matrix. Twomey (1977) recommends selecting the smallest value of γ which leads to a residual fit $\sum_i \epsilon_i^2$ which is a safe upper estimate of the overall error in $\mathbf{g}$ due to all causes (experimental error, quadrature error, etc.). Though this criterion is useful for isolating the approximate magnitude of γ, it is insufficient to guarantee finding a solution or that the solution once found is positive definite. Other investigators (e.g., Yamamoto and Tanaka, 1969) have done simulation studies from which a "best" value of γ was determined, a value which was kept fixed for all subsequent analyses of experimental data. Since γ enters (7) in a manner such that elements of $\gamma\mathbf{H}$ are to be added to $\mathbf{A}^T\mathbf{S}_\epsilon^{-1}\mathbf{A}$ to produce the desired smoothing, King *et al.* (1978) based their selection of γ on the magnitude of $\gamma H_{kj}/(\mathbf{A}^T\mathbf{S}_\epsilon^{-1}\mathbf{A})_{kj}$, rather than the magnitude of γ alone. The sensitivity of constrained linear inversions to the selection of the Lagrange multiplier will be demonstrated in the following sections for the case of inferring columnar aerosol size distributions from spectral aerosol optical depth measurements. It will be shown that it is convenient to vary $\gamma_{\text{rel}} \equiv \gamma H_{11}/(\mathbf{A}^T\mathbf{S}_\epsilon^{-1}\mathbf{A})_{11}$ in the range 10^{-3} to 5 until a range of values of γ_{rel} is reached for which all elements of $\mathbf{f}$ are positive (i.e., negative values of the elements of $\mathbf{f}$ constitute an unphysical solution). This represents the addition of an additional constraint which, like the smoothness constraint, is necessary to select a physical solution among the family of solutions which satisfy (3). In the sections which follow an iterative method will be described whereby an initial estimate of the solution is modified until the final solution satisfies both the positivity constraint *and* the constraint that the solution satisfy (3) to within the expected noise level of the measurements.

Once an appropriate value of γ has been determined, the solution covariance matrix can readily be obtained. Bevington (1969) shows that uncertainties in multiple regression problems are related to the symmetric matrix α, whose elements are given by

$$\alpha_{kl} = \frac{1}{2}\frac{\partial^2 Q}{\partial f_k \partial f_l}. \tag{9}$$

The matrix α is called the *curvature matrix* because of its relationship to the curvature of the Q hypersurface in coefficient space. The solution covariance matrix $\mathbf{S}$ is then obtained from the α^{-1} matrix, i.e.,

$$\mathbf{S} = \alpha^{-1}, \tag{10}$$

which, for constrained linear inversion, leads to

$$\alpha = \mathbf{A}^T\mathbf{S}_\epsilon^{-1}\mathbf{A} + \gamma\mathbf{H}, \tag{11}$$

$$\mathbf{S} = (\mathbf{A}^T\mathbf{S}_\epsilon^{-1}\mathbf{A} + \gamma\mathbf{H})^{-1}. \tag{12}$$

When $\gamma\mathbf{H}$ is replaced by the inverse of an *a priori* estimate of the solution covariance matrix, this equation becomes equivalent to the maximum likelihood solution obtained by Liebelt (1967) and Strand and Westwater (1968) and discussed in detail by Rodgers (1976).

If the uncertainties in the measurements are not known, they can be approximated from the data by

$$s^2 = \frac{1}{p-q}\sum_{i=1}^{p}\epsilon_i^2, \tag{13}$$

where s^2 is the sample variance for the regression fit and $p - q$ is a lower limit for the number of degrees of freedom after fitting p data points with q parameters. For this case the solution covariance matrix is given by

$$\mathbf{S} = s^2(\mathbf{A}^T\mathbf{A} + \gamma\mathbf{H})^{-1}. \tag{14}$$

Eqs. (12) and (14) are the equations for estimating the uncertainties in the inversion solution for constrained linear inversion problems. Eqs. (7) and (12) have been applied to spectral aerosol optical depth measurements obtained at the University of Arizona, since it is known that some of the optical depth measurements are more precise than others. For the case of aerosol optical depth measurements obtained at Goddard Space Flight Center the measurement errors are not known and thus inversions were performed using Eqs. (8), (13) and (14). Results of this analysis are presented and discussed in Section 4.

3. Determination of aerosol size distributions from spectral attenuation measurements

Under the assumption that atmospheric particulates can be modeled as a polydisperse collection of spherical particles with a single refractive index, the integral equation which relates the aerosol optical depths $\tau_a(\lambda)$ to an aerosol size distribution can be written in the form

$$\tau_a(\lambda) = \int_0^\infty \pi r^2 Q_{\text{ext}}(r, \lambda, m) n_c(r) dr. \tag{15}$$

In this expression r is the particle radius, λ the wavelength of incident illumination, m the complex refractive index of the aerosol particles, $Q_{\text{ext}}(r, \lambda, m)$ the extinction efficiency factor from Mie theory, and $n_c(r)$ the columnar aerosol size distribution, that is, the number of particles per unit area per unit radius interval in a vertical column through the atmosphere.

In order to determine $n_c(r)$ from spectral measurements of $\tau_a(\lambda)$, King *et al.* (1978) let $n_c(r) = h(r)f(r)$, where $h(r)$ is a rapidly varying function of r, while $f(r)$ is more slowly varying. With this substitution, Eq. (15) becomes

$$\tau_a(\lambda) = \int_{r_a}^{r_b} \pi r^2 Q_{ext}(r, \lambda, m)h(r)f(r)dr$$

$$= \sum_{j=1}^{q} \int_{r_j}^{r_{j+1}} \pi r^2 Q_{ext}(r, \lambda, m)h(r)f(r)dr, \quad (16)$$

where the limits of integration have been made finite with $r_1 = r_a$ and $r_{q+1} = r_b$. If $f(r)$ is assumed constant within each coarse interval, a system of linear equations of the form of (3) results, where the elements are given by

$$\left.\begin{aligned} g_i &= \tau_a(\lambda_i), && i = 1, 2, \ldots, p \\ A_{ij} &= \int_{r_j}^{r_{j+1}} \pi r^2 Q_{ext}(r, \lambda_i, m)h(r)dr, && j = 1, 2, \ldots, q \\ f_j &= f(r_j \leqslant r \leqslant r_{j+1}) \end{aligned}\right\}. \quad (17)$$

Initially a zeroth-order weighting function $h^{(0)}(r)$ is assumed in (17) from which first-order $f_j^{(1)}$ values are computed with the aid of (7) or (8). The first-order solution vector components $f_j^{(1)}$ are assumed to be valid at the geometric mean radius of each of the coarse intervals [*viz.*, $\bar{r}_j = (r_j r_{j+1})^{1/2}$], from which the first-order indicial function $f^{(1)}(r)$ is obtained by connecting straight line segments on an $f^{(1)}(r)$ vs log$r$ scale. Since $f^{(1)}(r)$ represents a modifying factor to the assumed form of $h^{(0)}(r)$, the $f^{(1)}(r)$ values are then used to calculate a first-order weighting function, $h^{(1)}(r) = h^{(0)}(r)f^{(1)}(r)$, which better represents the size distribution than the initially assumed weighting function. The first-order weighting function is then substituted back into (17) from which a second-order $\mathbf{f}^{(2)}$ is obtained through (7) or (8). This iterative procedure is continued until a stable result is obtained (Herman *et al.*, 1971; King *et al.*, 1978), but in no instance are more than eight iterations performed.

For the results presented in this paper, the initial weighting functions were assumed to have the form of a Junge (1955) size distribution, given by

$$h^0(r) = r^{-(\nu^*+1)}. \quad (18)$$

Several different values of ν^* are used to calculate the zeroth-order weighting function and the final results after successive iterations are intercompared. King *et al.* (1978) showed that the final results are usually insensitive to the initial estimates of the size distribution, even when the size distribution deviates markedly from a Junge distribution. The only difficulty which normally arises is in selecting the radius range having the major contribution to the measurements.

The sensitivity of spectral attenuation measurements to the radii limits and refractive index assumed in the inversion has previously been discussed (King *et al.*, 1978). There it was shown that the refractive index sensitivity is quite weak, affecting the inverted size distribution slightly by shifting its magnitude and radii while maintaining its overall *shape*. As a consequence, all inversions were performed assuming the complex refractive index of the aerosol particles was wavelength and size independent and given by $m = 1.45 - 0.00i$.

Phillips' (1962) second derivative smoothing constraint has been adopted in the present investigation. For a quadrature of equal division, the corresponding smoothing matrix $\mathbf{H}$ is given by (Twomey, 1963)

$$\mathbf{H} = \begin{pmatrix} 1 & -2 & 1 & 0 & 0 & & & & \\ -2 & 5 & -4 & 1 & 0 & 0 & & & \\ 1 & -4 & 6 & -4 & 1 & 0 & & & \\ 0 & 1 & -4 & 6 & -4 & 1 & 0 & & \\ & & & \ddots & & & & & \\ & & & & 0 & 1 & -4 & 5 & -2 \\ & & & & & 0 & 1 & -2 & 1 \end{pmatrix}. \quad (19)$$

Since this matrix is singular no corresponding inverse exists. Eqs. (7) and (12) are therefore consistent with the optimal estimation equations of Strand and Westwater (1968) and Rodgers (1976) where no *a priori* information exists on either the solution vector or its covariance matrix. Unlike the temperature sounding problem in which a vast quantity of information exists from past data, aerosol size distributions are more uncertain and variable. This necessitates the use of constrained linear inversions where an appropriate value of γ must be selected.

4. Selection of the Lagrange multiplier

The method for determining the columnar aerosol size distribution described in the preceding sections has been carried out at the University of Arizona since August 1975 and at Goddard Space Flight Center since July 1980. At the University of Arizona the relative irradiance of the directly transmitted sunlight was measured at selected wavelengths during the course of each cloud-free day from which the total optical depth of the atmosphere was determined using the Bouguer-Langley method (see, e.g., Shaw *et al.*, 1973). From the spectral variation of total optical depth the ozone absorption optical depths, and hence total ozone content of the atmosphere, have been derived by the method of King and Byrne (1976). The aerosol optical depth for each day and wavelength was determined by subtracting the molecular scattering and estimated ozone absorption contributions from the total optical depth. The variance in the daily aerosol optical depth for each wave-

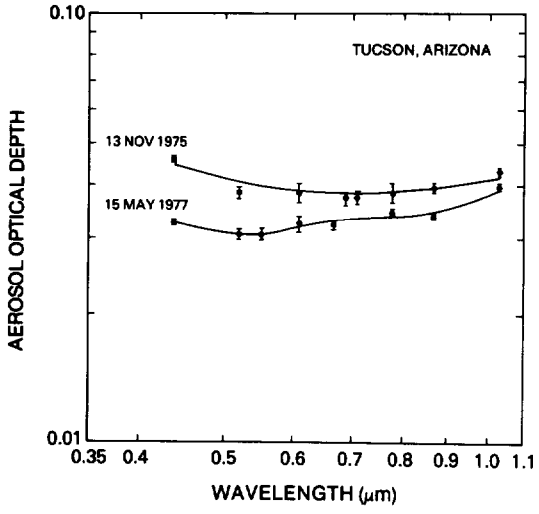

FIG. 1. Aerosol optical depth as a function of wavelength for Tucson, Arizona on 13 November 1975 and 15 May 1977. The smooth curves represent the regression fit to the data using the inverted size distributions.

length was obtained from the sum of the variances in the total optical depth and the ozone optical depth, both of which were estimated by the method of propagation of errors (see King and Byrne, 1976). A representative selection of aerosol size distribution results obtained at the University of Arizona has previously been presented and discussed (King *et al.*, 1978), together with a discussion of the relative frequency of occurrence of various types of distributions. In that article we discussed the sensitivity of spectral attenuation measurements to the radii limits of maximum sensitivity and to the refractive index of the aerosol particles assumed in the inversion. In the present paper emphasis will be placed on the sensitivity of constrained linear inversions to the selection of γ, the necessity of weighting the kernel by a modifying function $h(r)$, and the resulting uncertainties in the inversion solution.

Fig. 1 illustrates the observed aerosol optical depths and corresponding standard deviations for 13 November 1975 and 15 May 1977. The solid curves represent the regression fit to the $\tau_a(\lambda)$ measurements using the inverted size distributions presented below (i.e., the direct problem $\mathbf{g} = \mathbf{Af}$). In performing the inversions on these data the statistical errors in the measurements are assumed uncorrelated but known to be unequal. As a consequence, the measurement covariance matrix $\mathbf{S}_\epsilon$ becomes diagonal with elements given by $S_{\epsilon_{ij}} = \sigma^2_{\tau_a}(\lambda_i)\delta_{ij}$, where δ_{ij} is the Kronecker delta function. With $\mathbf{S}_\epsilon$ defined in this manner, Eq. (7) is equivalent to making a weighted least-squares fit to the data subject to a constraint.

In applying the inversion procedure described in the preceding section, several different initial Junge distribution parameters ν^* are assumed in formulating the zeroth-order weighting functions $h^{(0)}(r)$ so that the results after subsequent iterations can be intercompared. A best-fit value for the Ångström wavelength exponent α is determined from the observed values of $\tau_a(\lambda)$ by making a linear least-squares fit to Ångström's (1929) empirical formula given by $\tau_a(\lambda) = \beta\lambda^{-\alpha}$. Inversions are then performed for three different values of the Junge distribution parameter ν^* (*viz.*, $\alpha + 1.5$, $\alpha + 2.0$, $\alpha + 2.5$).

For the 13 November 1975 data case (see Fig. 1) $\alpha = 0.07$, and thus inversions were performed using the initial values $\nu^* = 1.57$, 2.07 and 2.57. Fig. 2 illustrates the inverted size distribution as a function of iteration for the case where the initial value of $\nu^* = 2.57$. In lieu of $n_c(r)$ or, equivalently, dN_c/dr, the size distributions are presented in terms of $dN_c/d\log r$, representing the number of particles per unit area per unit log radius interval in a vertical column through the atmosphere. The curve marked with the open circles represents the initial guess for the size distribution while all remaining curves represent the inversion results after subsequent iterations. The curves labeled L (or R) should be referred to the ordinate scale on the left (or right) side of the figure.

Having selected the zeroth-order weighting function $h^{(0)}(r)$ to be a Junge distribution with $\nu^* = 2.57$, we computed the **A** matrix elements using (17), from which first-order $f_j^{(1)}$ values were computed with the aid of (7). Fig. 3a illustrates the solution vector elements $f_j^{(1)}$ as a function of γ_{rel}, where the various j

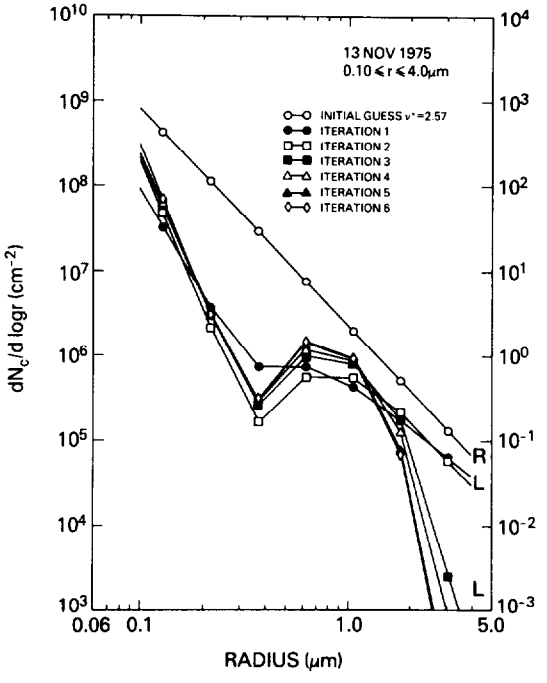

FIG. 2. Inverted size distribution as a function of iteration for 13 November 1975, where an initial guess of $\nu^* = 2.57$ was assumed. The curve labeled R applies to the right-hand scale and all other curves apply to the left-hand scale.

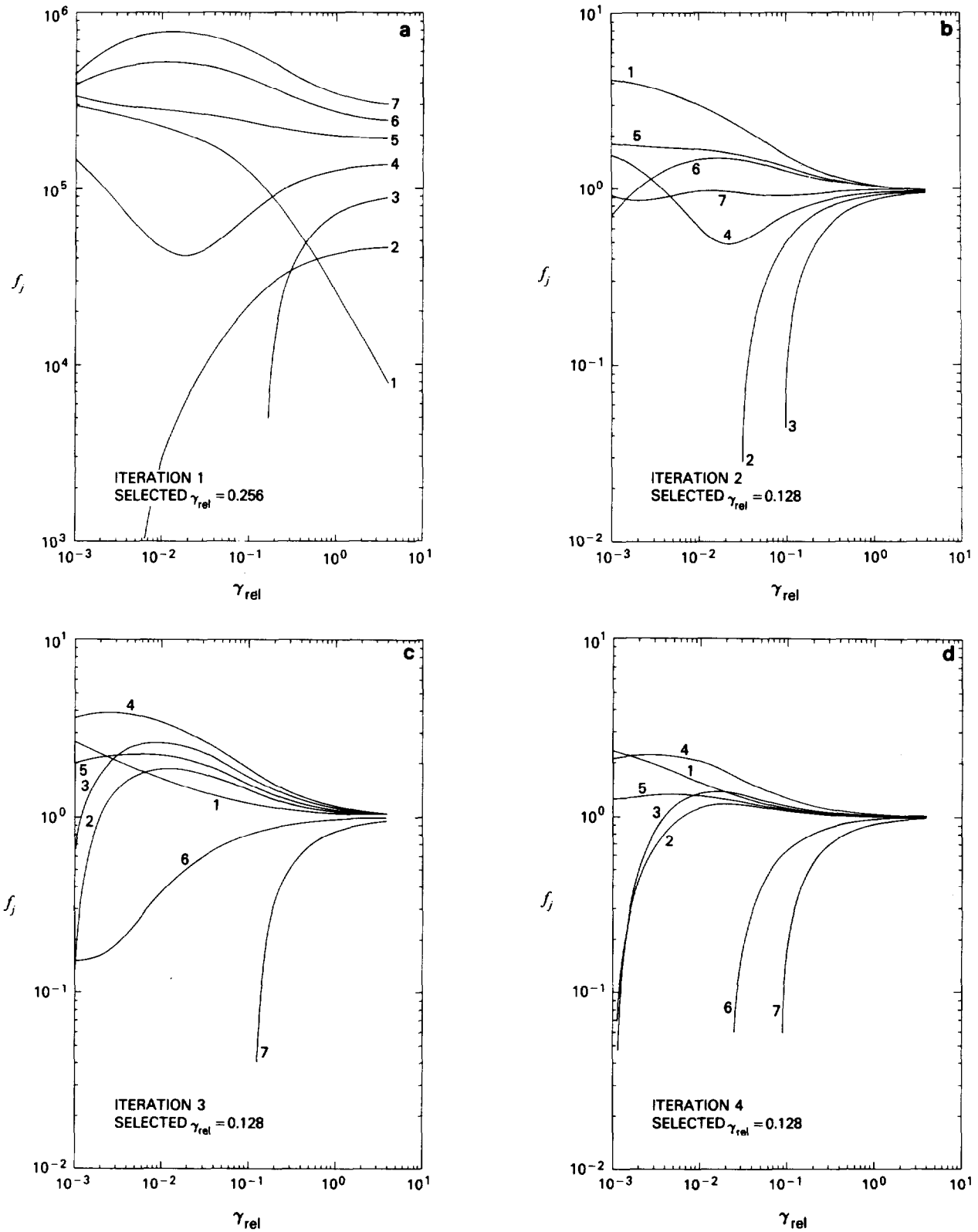

FIG. 3. Solution vector elements f_j as a function of γ_{rel} for measurements collected on 13 November 1975. The solution vector elements represent modifying factors to the assumed form of the size distribution, and the various j values correspond to radii at the midpoints of the jth log radius interval in Fig. 2. Part (a) corresponds to iteration 1, (b) to iteration 2, (c) to iteration 3 and (d) to iteration 4.

values correspond to radii $\bar{r}_j$ at the midpoints of the jth equal log radius interval in Fig. 2. Since $H_{11} = 1$ for the second derivative smoothing constraint, the relative Lagrange multiplier γ_{rel} is given by

$$\gamma_{rel} = \gamma/(\mathbf{A}^T\mathbf{S}_\epsilon^{-1}\mathbf{A})_{11} . \quad (20)$$

As $\gamma_{rel} \rightarrow \infty$ all solution vector elements approach asymptotic limits. The $j = 1$ radius point approaches within 5% of its asymptotic limit of 1.268×10^3 at $\gamma_{rel} \approx 300$, while all remaining solution vector elements approach within 5% of their asymptotic limits by $\gamma_{rel} \approx 3$. At $\gamma_{rel} = 0$, on the other hand, the least-squares solution exhibits large oscillations with $f_j^{(1)}$ values which are negative for $j = 1, 3, 6$ and 7. This undesirable (and unphysical) characteristic of least-squares solutions to Fredholm integral equations is well known. It is apparent from Fig. 3a that intermediate values of γ_{rel} produce a different kind of solution than those at either very large or very small values and thus the more oscillatory solutions which occur when $\gamma_{rel} = 0$ have been eliminated. Of those values of $f_j^{(1)}$ which were negative at $\gamma_{rel} = 0$, only the $j = 3$ value remains negative by the time $\gamma_{rel} = 10^{-3}$, not becoming positive until $\gamma_{rel} = 1.8 \times 10^{-1}$. The $j = 2$ solution, though positive at $\gamma_{rel} = 0$, becomes negative as γ_{rel} is increased until $\gamma_{rel} = 4.7 \times 10^{-3}$, after which point it becomes positive.

After examining numerous examples like Fig. 3a, not only for spectral attenuation measurements but also for angular light scattering (bistatic lidar) measurements, it has been determined that the important range for the Lagrange multiplier is the restricted range $10^{-3} \leqslant \gamma_{rel} \leqslant 5$. By doubling γ_{rel} throughout this range the solution vector elements can be examined by solving (7) for only 13 values of γ_{rel}. In Fig. 3a the smallest of these discrete values of γ_{rel} for which all elements of $\mathbf{f}^{(1)}$ are positive is $\gamma_{rel} = 0.256$.

In addition to being a positive function it is necessary for the inversion solution to satisfy (3) to within the expected noise level of the measurements. This is equivalent to requiring that the final solution simultaneously satisfy Twomey's (1977) criterion

$$Q_1 \leqslant E(Q_1), \quad (21)$$

where E denotes the expectation operator. For the University of Arizona cases in which it is assumed that $S_{\epsilon ij} = \sigma_{\tau_a}^2(\lambda_i)\delta_{ij}$, Eq. (21) is equivalent to requiring $Q_1 \leqslant p$, where $p = 8$ for both examples presented in Fig. 1. Since $Q_1 \geqslant 31.4$ for $\gamma_{rel} \geqslant 0.256$, Eq. (21) and the positivity constraint cannot both be satisfied after only one iteration. This is largely due to the initial guess being far from the final solution. Multiplying the $f_j^{(1)}$ values obtained for $\gamma_{rel} = 0.256$ by the initial Junge size distribution $h^{(0)}(\bar{r}_j)$ leads to the inversion solution illustrated in Fig. 2 for iteration 1. Note from Fig. 3a that the solutions for $j = 5$, 6 and 7 are virtually insensitive to γ_{rel} in the range $10^{-3} \leqslant \gamma_{rel} \leqslant 5$, but that $f_5^{(1)} < f_6^{(1)} < f_7^{(1)}$. This tendency to decrease the Junge slope below the value $\nu^* = 2.57$ is clearly evident in Fig. 2 for iteration 1. It is also apparent from Fig. 3a that the major instability in the solution vector was associated with $j = 2$ and 3. The reason for this is that the measurements contain sufficient information to construct a bimodal size distribution from an initial Junge distribution. This form of the size distribution is at odds with the smoothness constraint.

Since the new inversion better represents the size distribution than the initially assumed Junge distribution, the first-order weighting function $h^{(1)}(r)$ is substituted back into (17) from which a second-order $\mathbf{f}^{(2)}$ is obtained through (7). Fig. 3b illustrates the new solution vector elements $f_j^{(2)}$ as a function of γ_{rel}. Since the absolute magnitude of $h^{(1)}(r)$ deviates markedly from $h^{(0)}(r)$, as noted in Fig. 2, the magnitude of $(\mathbf{A}^T\mathbf{S}_\epsilon^{-1}\mathbf{A})_{11}$, and hence γ, deviates by 5.0×10^9 between iterations 1 and 2. This emphasizes the need to scale γ according to (20). As $\gamma_{rel} \rightarrow \infty$ all elements of $\mathbf{f}^{(2)}$ approach unity, representing a perfectly smooth (and over constrained) solution wherein the inversion solution would remain unaltered from that of the previous iteration. At $\gamma_{rel} \approx 1$ all $f_j^{(2)}$ values are within 5% of their asymptotic limit of unity. For the second iteration the major instability still remains with $j = 2$ and 3 since the inversion is trying to deepen the minimum between the two modes in the size distribution. For all remaining radii the inversion is relatively insensitive to the value of γ_{rel}. After selecting the minimum value (among the 13 discrete values) for which all elements of $f_j^{(2)}$ are positive (*viz.*, $\gamma_{rel} = 0.128$) and multiplying these values by the size distribution obtained from the previous iteration, the inversion solution illustrated in Fig. 2 for iteration 2 is obtained. Once again the regression fit to the data using the inverted size distribution lies outside the limits of the expected measurement errors (i.e., $Q_1 = 20.1 > p$). Therefore the inversion solution represented by iteration 2 in Fig. 2 represents a temporary solution (new first guess) and not an acceptable final solution.

This procedure is then repeated for iterations 3–8, where Figs. 3c and 3d illustrate the solution vector elements f_j as a function of γ_{rel} for iterations 3 and 4, respectively. The variations of f_j with γ_{rel} for iterations 5–8 (not illustrated) appear similar to those of iteration 4 (Fig. 3d). By the completion of iteration 2 the bimodal structure of the size distribution has clearly been established (cf. Fig. 2) and thus iterations 3–8 exhibit less instability in $j = 2$ and 3, concentrating instead on better defining the large particle end of the size distribution (*viz.*, $j = 6$ and 7).

Fig. 4 illustrates the magnitude of quadratics Q_1, Q_2 and Q as a function of γ_{rel} for iterations 1 and 6 on 13 November 1975. The curve labeled R applies

to the right-hand scale while all other curves apply to the left-hand scale. As γ_{rel} is increased, the value of Q_1 increases while Q_2 decreases, indicating that the requirement of smoothness is accomplished at the expense of the residual fit of the inversion solution to the measurements. Even though the least-squares solution ($\gamma = 0$) has an extremely small residual (Q_1) of 4.158×10^{-2} for iteration 1 and 6.275×10^{-2} for iteration 6, the solution vector **f** deviates markedly from the true solution **f'**. For iteration 1 it is necessary for $\gamma_{rel} \geq 0.181$ before all elements of the inverted solution vector are positive ($\gamma_{rel} \geq 0.027$ for iteration 6). Twomey (1965) has shown that the closeness of **f** to the true solution **f'** cannot be inferred by the closeness of the corresponding integral transform **Af** to **g**, measured by Q_1. Hoerl and Kennard (1970a) further showed that the minimum value of $|\mathbf{f}' - \mathbf{f}|$ is obtained at a value of $\gamma \neq 0$, and that the minimum value may be smaller than the least-squares solution for a wide range of γ values. In spite of this fact many investigators have chosen to find parameters of an assumed size distribution by minimizing Q_1. This is a more stringent approach than solving (7) or (8), for one is minimizing $Q = Q_1$ subject to the constraint that $f(r)$ has a predetermined functional form which may or may not be correct. Walters (1980) recently compared three methods of deriving an aerosol size distribution from spectral attenuation measurements, including constrained linear inversion [Eq. (8)] and parameter estimation, and concluded that constrained linear inversion offers the best chance of obtaining solutions in the absence of *a priori* information. It is important to recall that the quality that distinguishes inverse theory from the parameter estimation problem of statistics is that the unknowns are functions, not merely a handful of real numbers (Parker, 1977).

Returning to Fig. 4, one can see that if γ is chosen based on the criterion that $Q_1 \leq p$, equivalent to Twomey's (1977) suggestion that Q_1 be a safe upper estimate of all errors in **g**, one would require that $\gamma_{rel} \leq 0.051$ for iteration 1 and $\gamma_{rel} \leq 0.152$ for iteration 6. The values of γ_{rel} necessary to assure positive solutions are $\gamma_{rel} \geq 0.181$ for iteration 1 and $\gamma_{rel} \geq 0.027$ for iteration 6. Iteration 6 therefore constitutes an acceptable final solution if γ_{rel} is selected within the range $0.027 \leq \gamma_{rel} \leq 0.152$. If $Q_1 < p$, then some of the noise in **g** is being used in determining **f**. On the other hand, if $Q_1 > p$, then not all the information in **g** is being used to determine the solution vector **f**. Since γ_{rel} has been doubled within the range $10^{-3} \leq \gamma_{rel} \leq 5$, the maximum discrete value of γ_{rel} within the acceptable range $0.027 \leq \gamma_{rel} \leq 0.152$ is $\gamma_{rel} = 0.128$. The residual in the solution for iteration 6 ($\gamma_{rel} = 0.128$, $Q_1 = 7.9$) has been reduced by a factor of 4.0 over that obtained for iteration 1 ($\gamma_{rel} = 0.256$, $Q_1 = 31.4$). This suggests that the solution has been improved through iteration, as

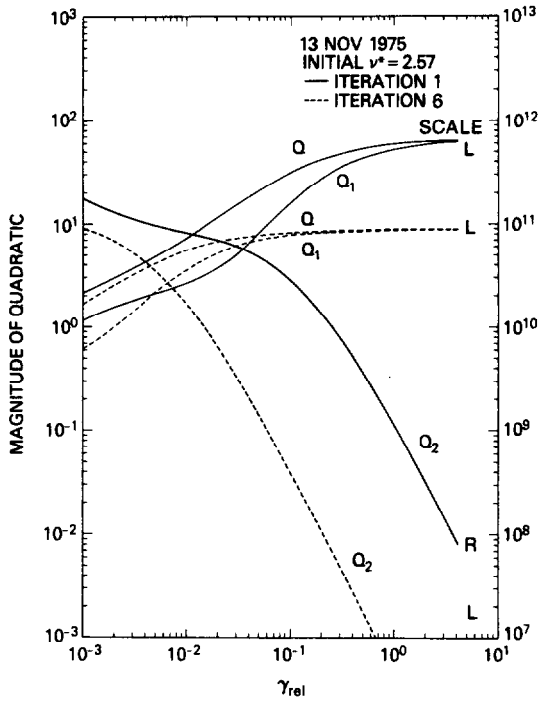

FIG. 4. Magnitude of quadratics Q_1, Q_2 and Q as a function of γ_{rel} for 13 November 1975. The curve labeled R applies to the right-hand scale and all other curves apply to the left-hand scale.

previously described, and that quadrature errors which contribute to Q_1 have also been reduced.

Fig. 2 presents the inversion solutions for iterations 1–6, where iteration 6 is the first iteration which simultaneously satisfies the positivity constraint and the criterion $Q_1 \leq p$. Iterations 7 and 8 had little difficulty satisfying both constraints and thus the largest value of γ_{rel} was selected (*viz.*, $\gamma_{rel} = 4.096$). The inversion solutions for these iterations as well as the final results obtained after successive iterations with $\nu^* = 1.57$ and 2.07 are virtually identical with those presented in Fig. 2 (iteration 6).

Once the optimum estimate of γ_{rel} has been determined, the covariances $S_{kl} = \sigma^2_{f_k f_l}$ are obtained from the elements of the solution covariance matrix **S**, given by (12). Fig. 5 illustrates the inverted size distribution and estimated standard deviations for 13 November 1975, where the corresponding regression fit to the $\tau_a(\lambda)$ measurements is shown as a solid curve in Fig. 1. As one would expect the uncertainties in the inverted size distribution become large as the particle radius becomes large since the information content of the measurements becomes small. In the minimum between the accumulation ($r \leq 0.37$ μm) and coarse particle ($r \geq 0.37$ μm) modes the error bars are often large for the same reason [see Fig. 9b of King *et al.* (1978) for an illustration of the kernel functions for a comparable bimodal size distribution case]. On many days with data similar to the present example, error bars in the intramodal region are

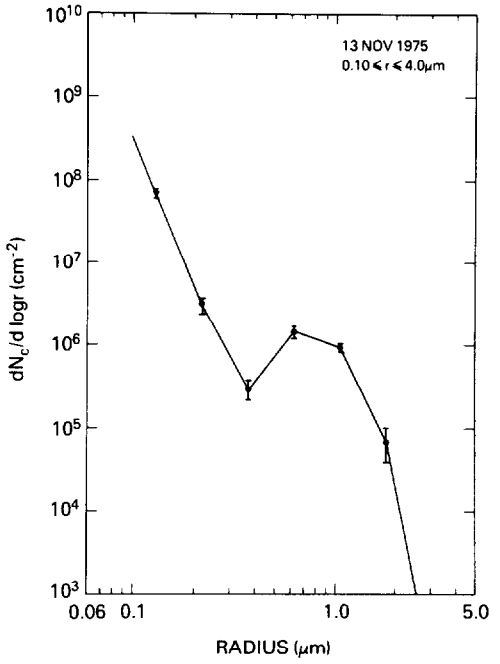

FIG. 5. Inverted size distribution and estimated standard deviations for 13 November 1975. The regression fit to the data using the inverted size distribution is illustrated in Fig. 1.

larger than in Fig. 5. For the smallest radii the relatively small error bars in Fig. 5 reflect the existence of sufficient information content that it would have been possible to perform the inversion using a small minimum radius r_a. Had the inversion been performed using an upper radius which is too large (or occasionally too small), instabilities develop such that subsequent iterations produce more and more particles at the larger radii (King *et al.*, 1978). All cases having initial weighting functions with $\nu^* = 1.57$ and 2.07 are similar to the one presented in Fig. 5 (with $\nu^* = 2.57$), where all three solutions lie within the error bars presented in Fig. 5.

On 15 May 1977 the spectral dependence of the aerosol optical depth was decidedly different than in the preceding example (cf. Fig. 1). In a similar manner to the method described above, an Ångström wavelength exponent was estimated from the data to be $\alpha = -0.21$, and thus inversions were performed using weighting functions having initial Junge parameters $\nu^* = 1.29$, 1.79 and 2.29. Fig. 6 illustrates the inverted size distribution as a function of iteration while Fig. 7 presents corresponding illustrations of the solution vector elements f_j as a function of γ_{rel}. Figs. 6 and 7 apply to the case where the initial value of $\nu^* = 1.79$.

Days for which the aerosol optical depths increase with wavelength invariably produce inverted size distributions which are relatively monodisperse, as is the case with the data on 15 May 1977. The most difficult type of aerosol optical depth data to invert are those which lead to relatively monodisperse size distributions since the radii which contribute to the spectral aerosol optical depth measurements are restricted to lie within a very narrow range. The data on 15 May 1977 were specifically selected because they clearly demonstrate that the inversion procedure is capable of dramatically perturbing the initial guess as required, and of obtaining a stable solution. The inversion of the 15 May 1977 data was performed at eight radii (i.e., $q = 8$) within the range $0.50 \leq r \leq 1.9$ μm, rather than $0.10 \leq r \leq 4.0$ μm as in the previous example.

At $\gamma_{rel} = 0$ the least-squares solution for iteration 1 again exhibits large oscillations with $f_j^{(1)}$ values which are negative for $j = 1$, 3, 5, 7 and 8. Not only are the coefficients incorrect with respect to sign but they are too large in absolute value. This is fundamentally due to the fact that the $\mathbf{A}^T\mathbf{S}_\epsilon^{-1}\mathbf{A}$ matrix has small eigenvalues, which in turn is a manifestation of a high degree of interdependence (nonorthogonality) of the kernels. As γ_{rel} is increased the small eigenvalues of $\mathbf{A}^T\mathbf{S}_\epsilon^{-1}\mathbf{A}$ are effectively increased by $\mathbf{A}^T\mathbf{S}_\epsilon^{-1}\mathbf{A} + \gamma\mathbf{H}$, whereas the large eigenvalues remain essentially unaltered. Of the five values of $f_j^{(1)}$ which were negative at $\gamma_{rel} = 0$, only the end points $j = 1$ and 8 remain negative by the time $\gamma_{rel} = 10^{-3}$, not becoming positive until $\gamma_{rel} = 7.2 \times 10^{-1}$ and 9.5

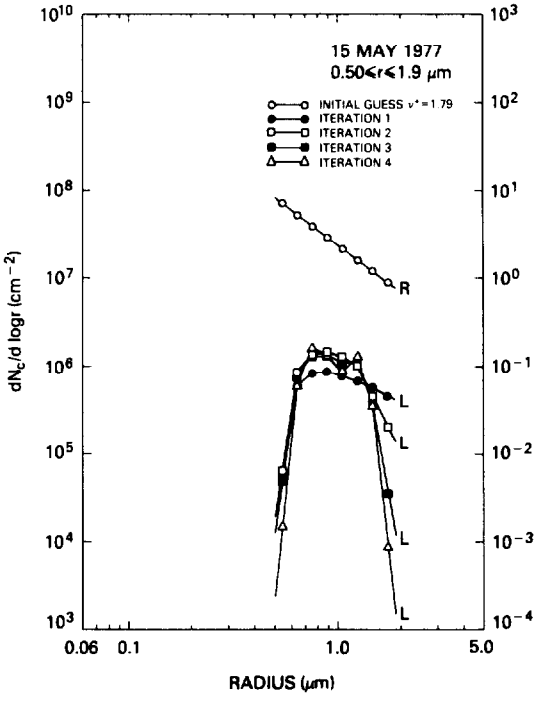

FIG. 6. Inverted size distribution as a function of iteration for 15 May 1977, where an initial guess of $\nu^* = 1.79$ was assumed. The curve labeled R applies to the right-hand scale and all other curves apply to the left-hand scale.

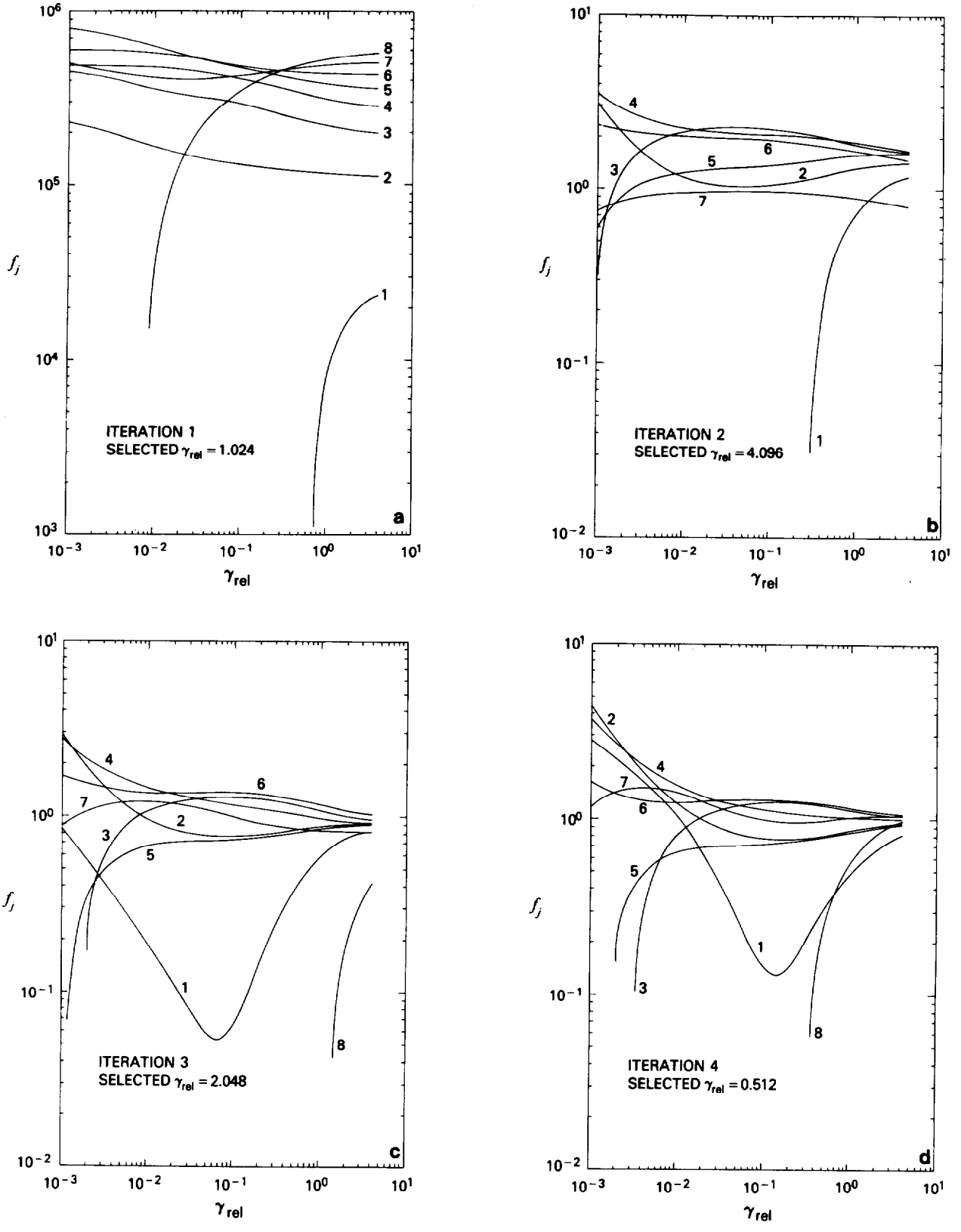

FIG. 7. As in Fig. 3 except for measurements collected on 15 May 1977.

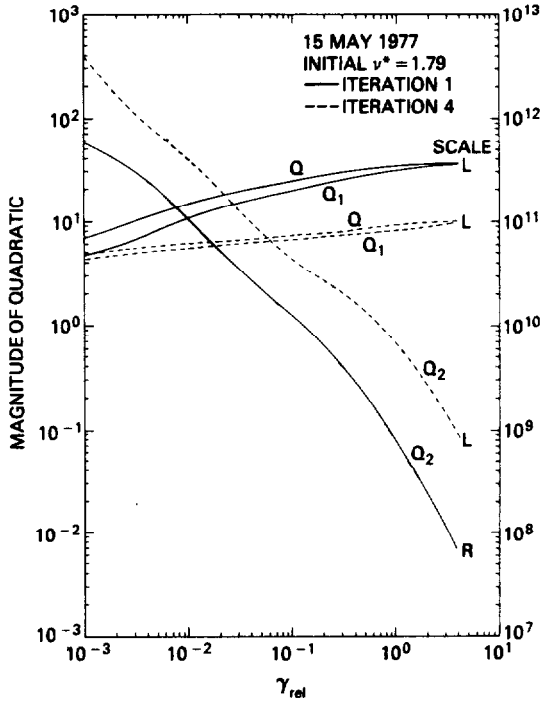

FIG. 8. As in Fig. 4 except for measurements collected on 15 May 1977.

$\times 10^{-3}$, respectively. As the Lagrange multiplier is further increased the constraint increasingly dominates the solution. Since γ_{rel} has been doubled within the range $10^{-3} \leqslant \gamma_{rel} \leqslant 5$, the minimum value of γ_{rel} for which all elements of $\mathbf{f}^{(1)}$ are positive is $\gamma_{rel} = 1.024$. Since $Q_1 = 31.8 > p$ for $\gamma_{rel} = 1.024$ the solution vector $\mathbf{f}^{(1)}$ represents a temporary solution, not an acceptable final solution. Multiplying the $\mathbf{f}^{(1)}(\bar{r}_j)$ values obtained for $\gamma_{rel} = 1.024$ by the initial Junge size distribution leads to the inversion illustrated in Fig. 6 for iteration 1.

After substituting the first-order weighting function $h^{(1)}(r)$ back into (17) a second-order solution vector $\mathbf{f}^{(2)}$ is obtained through (7). Unlike any of the previous examples the inversion was unable to obtain a positive solution for all elements of $f_j^{(2)}$ as γ_{rel} was varied. Since the $j = 8$ coefficient was still negative at $\gamma_{rel} = 4.096$, the $j = 6$ and 7 coefficients were used to extrapolate to $j = 8$ linearly on a $\log f_j$ vs j scale. In this way the unphysical value of $f_8^{(2)}$ was artificially made positive, leading to the solution presented in Fig. 6 for iteration 2. This procedure is then repeated for iterations 3 and 4, presented in Figs. 7c and 7d, except now it is possible to obtain positive values for all elements of $\mathbf{f}$ at several values of γ_{rel} within the range $10^{-3} \leqslant \gamma_{rel} \leqslant 5$. Fig. 6 presents the inversion solution for iterations 3 and 4, where $\gamma_{rel} = 2.048$ and 0.512 were selected, respectively. In this example iteration 4 is the first iteration for which both the positivity constraint and the condition of Eq. (21) are simultaneously satisfied. Further iterations produce results essentially identical to Fig. 6 (iteration 4).

The quadratics Q_1, Q_2 and Q are presented in Fig. 8 as a function of γ_{rel} for iterations 1 and 4 on 15 May 1977. The residual in the solution for iteration 4 ($\gamma_{rel} = 0.512$, $Q_1 = 7.7$) has been reduced by a factor of 4.1 over that obtained for iteration 1 ($\gamma_{rel} = 1.024$, $Q_1 = 31.8$). For iteration 4 the value of Q_1 at $\gamma_{rel} = 0$ is 4.415 and thus the residual has not been inflated to an unreasonable value at $\gamma_{rel} = 0.512$. The smoothness quadratic Q_2, on the other hand, has been reduced by over two orders of magnitude such that $|\mathbf{f}' - \mathbf{f}|$ is smaller than in the least-squares case. Hoerl and Kennard (1970a) have proven that, at least when $\mathbf{H} = \mathbf{I}$, there *always* exists a $\gamma > 0$ such that $|\mathbf{f}' - \mathbf{f}|$ is smaller than in the least-squares case. They further showed that this effect quite often exists over a wide range of γ values. If we had chosen γ based solely on the criterion that $Q_1 = p$, the value of γ_{rel} for iteration 1 would have been $\gamma_{rel} = 4.7 \times 10^{-3}$, a value for which $f_1^{(1)}$ and $f_8^{(1)}$ are negative (cf. Fig. 7a). By iterating and thereby reducing the quadrature errors associated with assuming $f(r)$ a constant within each coarse interval, the value of Q_1 for iteration 4 has been reduced to $Q_1 \approx p$. Although it has been our experience that the magnitude of quadratic Q_1 decreases with subsequent iterations due to a reduction in quadrature errors and errors associated with a smoothness constraint initially at

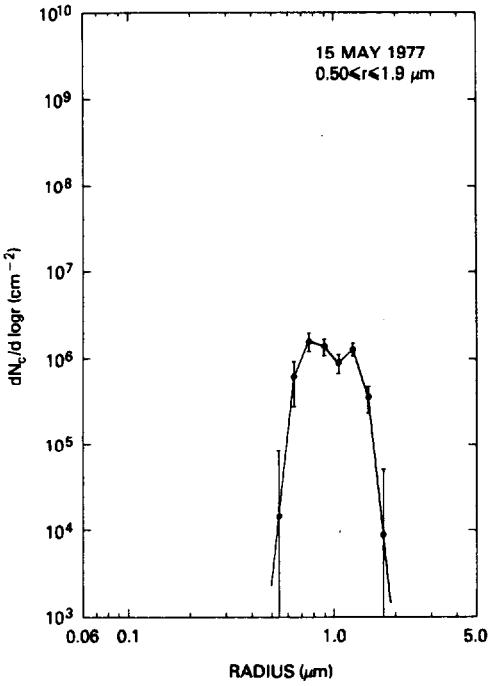

FIG. 9. Inverted size distribution and estimated standard deviations for 15 May 1977. The regression fit to the data using the inverted size distribution is illustrated in Fig. 1.

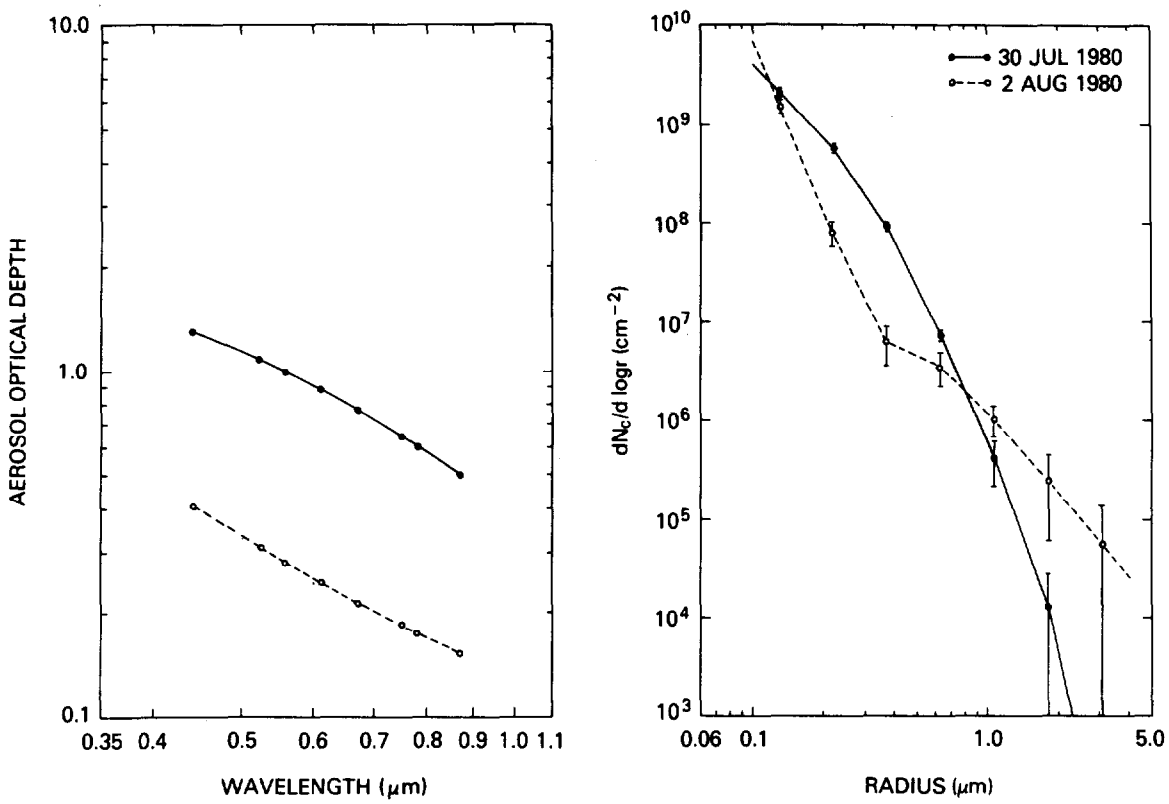

FIG. 10. Observed aerosol optical depths and estimated size distributions for measurements collected at Goddard Space Flight Center on 30 July 1980 and 2 August 1980. The curves on the left indicate the regression fit to the data using the inverted size distributions.

odds with the data, it is not always the case that Q_1 approaches p after repeated iterations. We have observed many instances in which $Q_1 < p$ for all values of γ. This is at least partly due to measurement correlations which contribute to the magnitude of Q_1 [cf. Eq. (5)] but which have been neglected in our analysis.

Fig. 9 illustrates the inverted size distribution and estimated standard deviations for 15 May 1977, where the corresponding fit to the $\tau_a(\lambda)$ measurements is shown as a solid curve in Fig. 1. The uncertainties in the inverted size distribution are large at both the upper and lower ends of the radius range. This is to be expected from the kernel function for cases where the inverted size distribution is relatively monodisperse (King *et al.*, 1978). Had the inversion been performed using a wider radius range than the one used here it would have been impossible to obtain a solution which was everywhere positive. All cases having initial weighting functions with $\nu^* = 1.29$ and 2.29 are similar to the result presented in Fig. 9 (where $\nu^* = 1.79$). All three solutions lie well within the error bars presented in Fig. 9.

At Goddard Space Flight Center the relative irradiance of the directly transmitted solar radiation was measured during the course of selected cloud-free days with a portable multi-wavelength solar radiometer. The time-dependent total optical depth of the atmosphere was determined with repeated application of the Lambert-Beer law, where the intercept voltage level (proportional to the extraterrestrial solar irradiance) was determined using the Bouguer-Langley method at Mauna Loa Observatory. The aerosol optical depth for each time and wavelength was subsequently determined by subtracting the molecular scattering and ozone absorption contributions from the total optical depth. Although a constant, climatological value for total ozone content was assumed, the error introduced by this assumption is small since the aerosol optical depths thus obtained are large compared to any uncertainty in the ozone optical depths.

Fig. 10 illustrates the spectral optical depth measurements and corresponding size distributions for 30 July 1980 and 2 August 1980. Since uncertainties and correlations in the measurements were not known, the measurement errors were assumed equal and uncorrelated and thus inversions were performed using Eqs. (8), (13) and (14). In all instances the sensitivity to the initial weighting function $h^{(0)}(r)$ was negligible. The negative curvature in the size distribution on 30 July 1980 is associated with the ne-

gative curvature in the input data, whereas the subtle bimodal characteristics of the 2 August 1980 size distribution are due to the positive curvature in the input data, particularly at the longer wavelengths. The increasingly large standard deviations in the size distribution at $r \geq 2.0$ μm are to be expected from the decreasing information content of the kernel functions for these radii. However, inversions performed only out to $r_b = 2.0$ μm often lead to unsatisfactory and unstable solutions (King *et al.*, 1978). The selection of the Lagrange multiplier and the updating of the initial size distribution estimate through iteration were accomplished in the same manner as previously described, except now Eq. (21) takes the form $Q_1 \leqslant E(\sum_i \epsilon_i^2) = e^2$.

5. Summary and conclusions

Results have been presented which demonstrate the sensitivity of constrained linear inversions to the selection of the Lagrange multiplier. Since γ enters (7) in a manner such that elements of $\gamma\mathbf{H}$ are to be added to $\mathbf{A}^T\mathbf{S}_\epsilon^{-1}\mathbf{A}$ to produce the desired smoothing, a relative Lagrange multiplier γ_{rel} is introduced since the magnitude of γ_{rel} is of importance and not the magnitude of γ alone. Inversion formulas (7) and (8) have been applied to the problem of determining the columnar aerosol size distribution from spectral aerosol optical depth measurements. An iterative method of solution is presented whereby an estimate of the size distribution is included in the elements of the **A** matrix. With this procedure, the inverted solution vector **f** amounts to a modifying function to the assumed form of the size distribution.

As demonstrated in Figs. 3 and 7 there are frequently regions of the Lagrange multiplier where all of the solution values f_j are positive and other regions where one or more f_j values are negative. The values of f_j for some radii values may periodically go negative and become positive again at larger values of γ_{rel}. After selecting a value for γ_{rel} in a region where all elements of the solution vector are positive and recomputing the **A** matrix elements, the solution vector for subsequent iterations becomes less sensitive to γ_{rel}. If the radii limits are very far from the optimum ones, however, it may not be possible to obtain a solution where all elements of **f** are positive. By doubling γ_{rel} in the range 10^{-3} to 5 until a range of values of γ_{rel} is reached for which all elements of **f** are positive, it is necessary to perform at most 13 matrix inversions per iteration per initial size distribution estimate. The inversion method is therefore quite rapid, requiring only about 1.0 s of execution time on an IBM 3081 computer.

In addition to the positivity constraint it is necessary for the final solution to satisfy the original integral equation to within the expected noise level of the measurements. If the initial estimate of the solution is very far from the final solution, then this criterion and the requirement of positivity cannot simultaneously be satisfied. Through iterative adjustment of the first guess we demonstrate how both criteria can ultimately be satisfied, thereby narrowing the domain of nonuniqueness in the solution. If the uncertainties in the measurements are unusually large, then it is relatively easy to obtain inversion solutions which satisfy both criteria but the uncertainties in the solution are large. On the other hand, measurement errors which are estimated unrealistically small may preclude being able to obtain a final solution which satisfies both constraints. It is therefore important that realistic uncertainties be assigned to the data before performing an inversion.

Once an appropriate value of γ has been determined, the variance and covariance in the solution can be estimated from the elements of the solution covariance matrix **S**. Eq. (12) has been applied to spectral aerosol optical depth measurements obtained at the University of Arizona, since it is known that some of the measurements are more precise than others. At Goddard Space Flight Center the measurement errors are unknown and thus inversions and error analyses were performed using Eqs. (8), (13) and (14). Results of this analysis, presented in Figs. 5 and 9 for the University of Arizona and Fig. 10 for Goddard Space Flight Center, show that the variances in the solution vector are large for radii where the information content of the measurements is small. Results further indicate that as γ increases the correlation between various values of f_j increases.

Various automatic procedures which have been used in the literature for selecting the "best" value for the Lagrange multiplier give little insight into the structure of the solution and its sensitivity to the data being analyzed. By computing **f**, Q_1 and Q_2 as a function of γ and displaying the results, considerable insight into the solution can be obtained. For physical problems in which additional *a priori* information exists on the solution (such as the requirement that the size distribution be positive or that the absolute temperature exceed some minimum temperature such as 160K) such information should be incorporated in the inversion to help restrict the possible domain of the solution. Complete elimination of the nonuniqueness of the solution is of course not possible.

Acknowledgments. The author is grateful to Drs. D. M. Byrne and M. J. Munteanu for carefully reading the original manuscript and for providing helpful comments, and to Drs. R. S. Fraser and Y. J. Kaufman for collecting the optical thickness measurements at Goddard Space Flight Center. The author would further like to thank an anonymous referee whose careful review and comments led to improvements in the manuscript.

REFERENCES

Ångström, A., 1929: On the atmospheric transmission of sun radiation and on dust in the air. *Geogr. Ann.*, **11**, 156–166.

Bevington, P. R., 1969: *Data Reduction and Error Analysis for the Physical Sciences.* McGraw-Hill, 336 pp.

Byrne, D. M., 1978: Remote detection of atmospheric particulates using a bistatic lidar. Ph.D. dissertation, University of Arizona, 144 pp.

Dave, J. V., 1971: Determination of size distribution of spherical polydispersions using scattered radiation data. *Appl. Opt.*, **10**, 2035–2044.

DeLuisi, J. J., and C. C. Mateer, 1971: On the application of the optimum statistical inversion technique to the evaluation of Umkehr observations. *J. Appl. Meteor.*, **10**, 328–334.

Glasco, V. B., and Yu. M. Timofeyev, 1968a: The solution of the thermal sounding problem for the atmosphere using the regularization method. *Izv. Atmos. Oceanic Phys.*, **4**, 170–174.

——, and ——, 1968b: Possibilities of the regularization method in solving the problem of atmospheric thermal sounding. *Izv. Atmos. Oceanic Phys.*, **4**, 713–718.

Herman, B. M., S. R. Browning and J. A. Reagan, 1971: Determination of aerosol size distributions from lidar measurements. *J. Atmos. Sci.*, **28**, 763–771.

Hoerl, A. E., and R. W. Kennard, 1970a: Ridge regression: Biased estimation for nonorthogonal problems. *Technometrics*, **12**, 55–67.

——, and ——, 1970b: Ridge regression: Applications to nonorthogonal problems. *Technometrics*, **12**, 69–82.

Junge, C. E., 1955: The size distribution and aging of natural aerosols as determined from electrical and optical data in the atmosphere. *J. Meteor.*, **12**, 13–25.

King, M. D., and D. M. Byrne, 1976: A method for inferring total ozone content from the spectral variation of total optical depth obtained with a solar radiometer. *J. Atmos. Sci.*, **33**, 2242–2251.

——, ——, B. M. Herman and J. A. Reagan, 1978: Aerosol size distributions obtained by inversion of spectral optical depth measurements. *J. Atmos. Sci.*, **35**, 2153–2167.

Liebelt, P. B., 1967: *An Introduction to Estimation Theory.* Addison-Wesley, 273 pp.

Parker, R. L., 1977: Understanding inverse theory. *Annual Review of Earth and Planetary Sciences*, Vol. 5, Annual Reviews, Inc., 35–64.

Phillips, D. L., 1962: A technique for the numerical solution of certain integral equations of the first kind. *J. Assoc. Comput. Mach.*, **9**, 84–97.

Reagan, J. A., D. M. Byrne, M. D. King, J. D. Spinhirne and B. M. Herman, 1980: Determination of the complex refractive index and size distribution of atmospheric particulates from bistatic-monostatic lidar and solar radiometer measurements. *J. Geophys. Res.*, **85**, 1591–1599.

Rodgers, C. D., 1970: Remote sounding of the atmospheric temperature profile in the presence of cloud. *Quart. J. Roy. Meteor. Soc.*, **96**, 654–666.

——, 1971: Some theoretical aspects of remote sounding in the earth's atmosphere. *J. Quant. Spectrosc. Radiat. Transfer*, **16**, 767–777.

——, 1976: Retrieval of atmospheric temperature and composition from remote measurements of thermal radiation. *Rev. Geophys. Space Phys.*, **14**, 609–624.

Shaw, G. E., J. A. Reagan and B. M. Herman, 1973: Investigations of atmospheric extinction using direct solar radiation measurements made with a multiple wavelength radiometer. *J. Appl. Meteor.*, **12**, 374–380.

Strand, O. N., and E. R. Westwater, 1968: Statistical estimation of the numerical solution of a Fredholm integral equation of the first kind. *J. Assoc. Comput. Mach.*, **15**, 104–114.

Tikhonov, A. N., 1963: On the solution of incorrectly stated problems and a method of regularization. *Dokl. Acad. Nauk SSSR*, **151**, 501–504.

Twomey, S., 1963: On the numerical solution of Fredholm integral equations of the first kind by the inversion of the linear system produced by quadrature. *J. Assoc. Comput. Mach.*, **10**, 97–101.

——, 1965: The application of numerical filtering to the solution of integral equations encountered in indirect sensing measurements. *J. Franklin Inst.*, **279**, 95–109.

——, 1977: *Introduction to the Mathematics of Inversion in Remote Sensing and Indirect Measurements.* Elsevier, 243 pp.

Walters, P. T., 1980: Practical applications of inverting spectral turbidity data to provide aerosol size distributions. *Appl. Opt.*, **19**, 2353–2365.

Wark, D. Q., and H. E. Fleming, 1966: Indirect measurements of atmospheric temperature profiles from satellites: I. Introduction. *Mon. Wea. Rev.*, **94**, 351–362.

Westwater, E. R., and O. N. Strand, 1968: Statistical information content of radiation measurements used in indirect sensing. *J. Atmos. Sci.*, **25**, 750–758.

Yamamoto, G., and M. Tanaka, 1969: Determination of aerosol size distribution from spectral attenuation measurements. *Appl. Opt.*, **8**, 447–453.

Yarger, D. N., 1970: An evaluation of some methods of estimating the vertical atmospheric ozone distribution from the inversion of spectral ultraviolet radiation. *J. Appl. Meteor.*, **9**, 921–928.